Numerical Simulation of Dynamic Centrifuge Tests on Concrete Faced Rockfill Dam

Muhsin Acar, S.M.ASCE[1]; Ozgun A. Numanoglu, S.M.ASCE[2];
and Youssef M. A. Hashash, Ph.D., P.E., F.ASCE[3]

[1]Graduate Student, Dept. of Civil and Environmental Engineering, Univ. of Illinois at Urbana–Champaign, Urbana, IL 61801. E-mail: macar2@illinois.edu
[2]Graduate Student, Dept. of Civil and Environmental Engineering, Univ. of Illinois at Urbana–Champaign, Urbana, IL 61801. E-mail: numanog2@illinois.edu
[3]Professor, Dept. of Civil and Environmental Engineering, Univ. of Illinois at Urbana–Champaign, Urbana, IL 61801. E-mail: hashash@illinois.edu

ABSTRACT

Seismic behavior of concrete faced rockfill dams (CFRDs) has not been sufficiently examined due to limited measured response in the field. This study presents results of numerical experiments (finite element analyses), which investigate effects of hysteretic damping and interface between rockfill and concrete face on the seismic behavior of CFRDs. The analyses use a recently developed, three-dimensional, distributed element plasticity soil model (I-soil) which allows flexible control over hysteretic behavior and can model both Masing and user-defined non-Masing type un/reloading. Numerical results are compared with centrifuge test data performed by others, including spectral response, and bending moment increments on the concrete face. The best estimates were obtained using non-Masing type un/reloading rules along with frictional interaction between concrete face and rockfill interface. These results suggest that the seismic response of CFRDs can be better simulated with proper characterization of hysteretic damping and interaction between different components of the dam body.

INTRODUCTION

Concrete faced rockfill dams (CFRDs) have become commonly preferable dam type by designers due to its variable advantages, such as less and easier field requirements for foundations, more flexible construction schedule, and great adaptability to the topography and inherent stability against earthquakes (Seo et al. 2009; C. Marulanda & Marulanda, 2015; Bayraktar and Kartal 2010; Wen et al. 2017). The design approaches of CFRDs have been based on empiricism and experience. Several recent incidents in which the concrete face slab cracked due to deformations occurred in the rockfill as a result of first reservoir fillings and/or an earthquake event point to the need for better estimating the behavior of CFRDs (Marulanda-Escobar & Marulanda-Posada, 2008; C. Marulanda & Marulanda, 2015). Even though it has been stated that CFRDs are reasonably safe against earthquakes because excess porewater pressure generation does not occur (Sherard and Cooke 1987), the seismic-induced deformations may cause serious damage to the concrete face. Such problems can be analyzed numerically to better understand the behavior of CFRDs under seismic loading conditions and to propose engineering solutions.

It is desirable to compare the results of numerical simulation studies on CFRDs with measured response to verify the reliability of the numerical tools. Such studies have remained limited due to lack of data recorded during an earthquake event. In this study, nonlinear dynamic finite element analyses of a CFRD numerical model are performed using LS-DYNA software (LSTC 2009) to estimate the measured behavior of a corresponding dynamic centrifuge tests.

The influence of: (1) un/reloading rules on modeling hysteretic response; and (2) interface between concrete slab and rockfill including welded and friction contact types on the dynamic behavior of CFRD are investigated.

CENTRIFUGE TESTS AND INSTRUMENTATION

The dynamic centrifuge tests that are used as a case study for this project has been conducted at the Korea Advanced Institute of Science and Technology (KAIST) centrifuge and earthquake simulator. 2-D cross section of the centrifuge model along with the dimensions and installed instrumentations are illustrated in Figure 1. There are 7 accelerometers (A), 8 strain gages (SG), and 2 laser displacement sensors (LDS) installed in the model. According to Kim et al. (2011), 4 strain gages (SG2, SG3, SG5, and SG6) did not provide data during the tests due to a problem in data acquisition system. The centrifugal acceleration employed for these tests is 40 g, which led to having a prototype CFRD model with a height, crest width and thickness of concrete face slab of 6.4 m, 0.9 m, and 0.042 m, respectively. The concrete face in the model was represented by a 3-mm thick high-density polyethylene (HDPE) with an elastic modulus of 1.2 GPa in model scale (Kim et al. 2011).

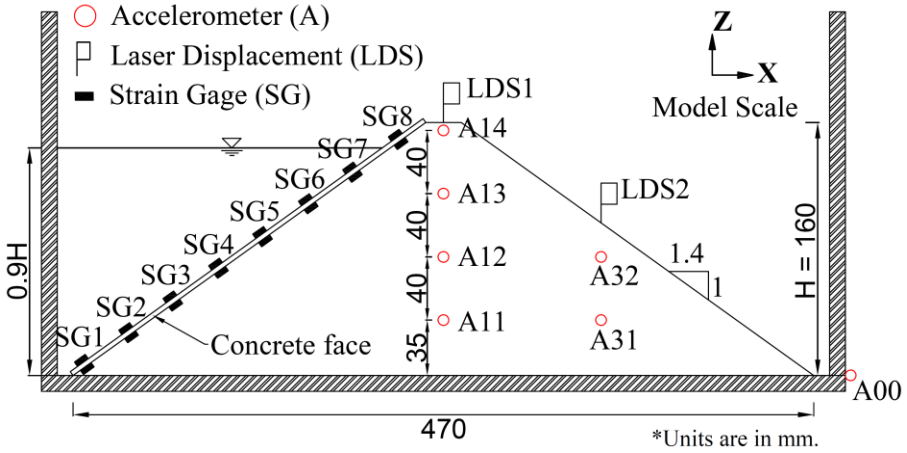

Figure 1: Layout of the centrifuge model along with instrumentation (reprinted from Kim et al. 2011).

Table 1: Properties of the baseline corrected motions recorded at the base of the container.

Test Name	PGA (g)	I_A (m/sec)	Motion Label
Test 01	0.090	0.06	T01
Test 02	0.130	0.18	T02
Test 03	0.171	0.31	T03
Test 04	0.213	0.50	T04
Test 05	0.282	0.83	T05
Test 06	0.365	1.29	T06
Test 07	0.417	2.51	T07
Test 08	0.439	2.99	T08
Test 09	0.549	3.63	T09

Nine dynamic tests (PGAs and Arias Intensity (I_A) ranging from 0.09g to 0.55g and 0.06 m/sec to 3.63 m/sec respectively) using the Ofunato earthquake record (M_S = 7.4, 1978) have

sequentially been carried out by Kim et al. (2011), The base motions from these tests (characteristics tabulated in Table 1) are used as base excitations in numerical simulations.

The rockfill material used in the centrifuge test was gathered from a real dam construction site in Korea to represent similar rockfill properties in the field. Particle gradation method was used to reduce the particle size of the rockfill, so that the rockfill material could be used in the centrifuge tests (Kim et al. 2011). After reducing the particle size of the rockfill for the centrifuge model, a specimen with a median particle size (D_{50}) of 2.54 mm and uniformity coefficient (C_u) of 17.25 were obtained. The particle size distribution of the rockfill used in the centrifuge experiments were compared with some coarse-grained specimens (C33D1, C50D2, and C50D3) presented in Menq (2003), which was developed to determine dynamic properties of coarse grained soils, and a good agreement was obtained (see Figure 2b). Friction angle (φ') of 43˚, cohesion (c) of 8 (kPa), and density (ρ) of 2100 (kg/m^3) were reported for the rockfill material by Kim et al. (2011). The shear wave velocity (V_S) profile of rockfill material used in the centrifuge test was obtained from resonant column test and the equation of $V_S = 100.4\,(\sigma'_{mean})^{0.24}$ was derived (Kim et al. 2011). The effective mean stress (σ'_{mean}) dependent V_s values representing the profile from the crest to base of the dam at maximum height cross section in prototype scale is plotted in Figure 2a.

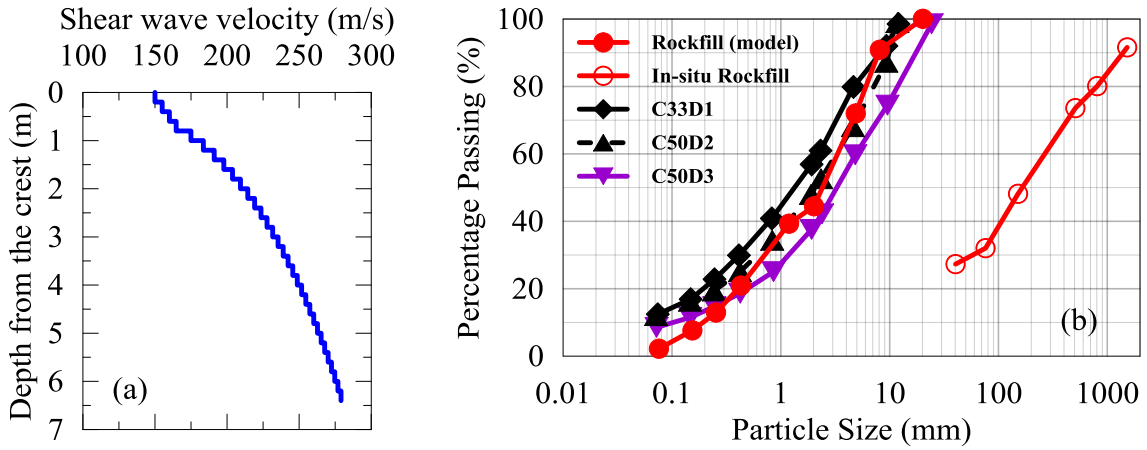

Figure 2: Properties of the rockfill: (a) Shear wave velocity vs depth from the crest at maximum cross section in prototype scale, (b) Particle size distribution of in-situ rockfill, the rockfill used in the model, and some specimens used in Menq (2003).

NUMERICAL MODEL

The configuration of the numerical model is shown in the Figure 3. The model consisted of 1957 eight-node brick elements using single point integration, including elements for rockfill, water and container, and 32 shell elements for concrete face slab. The reservoir was modeled in order to take account the dynamic effects of reservoir fluid on the dam response. The concrete face slab and water was modeled as linear elastic and elastic-fluid material models, respectively.

The bottom nodes of the model were vertically fixed and allowed to move in lateral direction (X-direction). Periodic boundary conditions were applied to the outermost nodes of the container elements at the same elevation in two degrees of freedom (in X and Z directions). All the nodes in the model were fixed in Y direction.

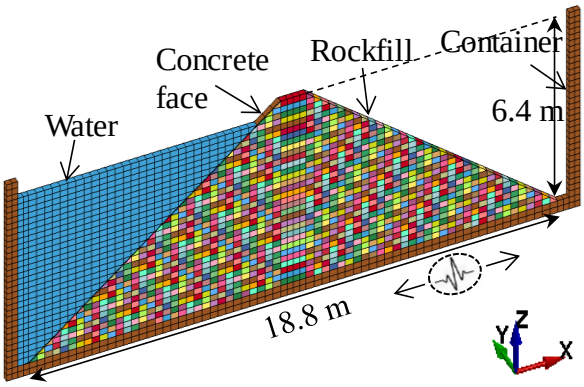

Figure 3: Configuration of the numerical model in prototype scale.

Constitutive Model: The numerical simulations use a three-dimensional effective stress soil model (I-soil) (Numanoglu, 2018) to describe important aspects of granular materials including normalized modulus reduction, hysteretic damping, shear induced volumetric (contraction - dilation) behavior in terms of strains and excess porewater pressures, and effective mean stress dependency of the stiffness and stress – strain behavior. The model uses distributed element modeling framework (Iwan 1967, Chiang and Beck 1994) whereby n number of nested elasto-plastic components are superimposed to obtain piecewise linearized shear stress – shear strain relation. The yield criteria for each nested component is defined via Drucker-Prager type conical yield surfaces. The monotonic part of the model is defined using a discrete point backbone curve as an input. The model provides flexible control over un/reloading rules including Masing type and non-Masing type un/reloading via constitutive modeling framework independent, generalized hysteresis modeling formulation in three-dimensional stress space (Numanoglu et al. 2017b). This formulation closely follows the un/reloading rules developed by Phillips and Hashash (2009) in which Masing un/reloading rules are modified using a reduction factor (MRDF model) of $F(\gamma_m) = p_1 - p_2\left(1-\frac{G_{\gamma_m}}{G_0}\right)^{p_3}$, where p_1, p_2 and p_3 are non-dimensional parameters to provide best fit with the target damping curve.

The effective mean stress dependency of the mobilized shear strength is achieved using 3D Drucker – Prager yield surfaces for nested components. In addition, the shear modulus is dependent on effective means stress using $G_0 = G_{0,ref}\left[\frac{\sigma'_{mean}-\sigma'_0}{\sigma'_{ref}}\right]^b$, where $G_{0,ref}$ = elastic shear modulus (shear modulus at the first segment of piecewise linear backbone curve) at a given reference effective mean stress (σ'_{ref}), σ'_0 = threshold value (a small quantity) below which stiffness is equal to $G_0 = G_{0,ref}\left[\frac{|\sigma'_0|}{\sigma'_{ref}}\right]^b$, and b = model coefficient characterizing the effective mean stress dependence of the shear modulus. The pressure dependent stiffness was activated by setting the parameter of b to 0.5 based on Richart et al. (1970).

The Rowe (1962) and its invariant form proposed by Nova and Wood (1979) are used to define the relation between volumetric and shear strains as $d\varepsilon_v^p = A_0(\eta_{pt}-\eta)d\varepsilon_q^p$, where A_0 is a scalar coefficient determining the rate of shear induced volumetric response, η is stress ratio

(deviatoric stress divided by effective mean stress), η_{pt} is phase transformation stress ratio, $d\varepsilon_v^p$ is plastic volumetric strain increment, and $d\varepsilon_q^p$ is plastic deviatoric strain increment. The model induces contractive behavior (decrease in void ratio) if ($\eta_{pt} - \eta > 0$) or dilatant behavior (increase in void ratio) if ($\eta_{pt} - \eta < 0$).

Several examples for the application of I-soil model in nonlinear site response analyses and 3-D soil-structure interaction analyses can be found in Baltaji et al. (2017) and Coleman et al. (2017). The next section describes the selection of dynamic properties of the rockfill and input parameters and curves for I-soil.

Dynamic Properties of the Rockfill and Constitutive Model Calibration: The normalized shear modulus reduction (G/G_{max}) and damping curves from Menq (2003) were used as the reference dynamic curves to define the shear stress-shear strain backbone curve for I-soil. The target shear strength of 43° is used at 3% shear strain level following the procedure described in Numanoglu et al 2017a. The at-rest coefficient of lateral earth pressure (K_0) were obtained using Jakey's equation of $K_0 = (1 - sin\varphi')$ (Jaky 1948). K_0 is also used in calculation of Poisson's ratio (ν) using the equation of $K_0 = \nu/(1-\nu)$. The resultant backbone curves are used for I-soil as an input curve at reference effective mean stresses. The GQ/H hyperbolic model (Groholski et al. 2016), which can control small strain soil stiffness and shear strength at large strains, was used to fit dynamic curves using DEEPSOIL v7.0 (Hashash et al. 2017), a 1-D nonlinear site response analysis software. Small strain shear modulus was calculated using $G_{max} = \rho V_s^2$, while τ_{max} was defined using $\tau_{max} = c + \sigma_v^{'} * tan(\varphi^{'})$.

Both Masing type and non-Masing type un/reloading rules were utilized to model the hysteretic damping for the rockfill. The reproduced hysteretic damping values with strain and the difference between Masing and non-Masing type models were demonstrated in Figure 4. Although the normalized modulus reduction curves for both cases agree very well with the reference curve, the hysteretic damping obtained with MRDF (non-Masing) procedure agrees well with both resonant column test results and reference curves by Menq (2003), while MR (Masing) procedure overestimates the damping of the soil at larger shear strains.

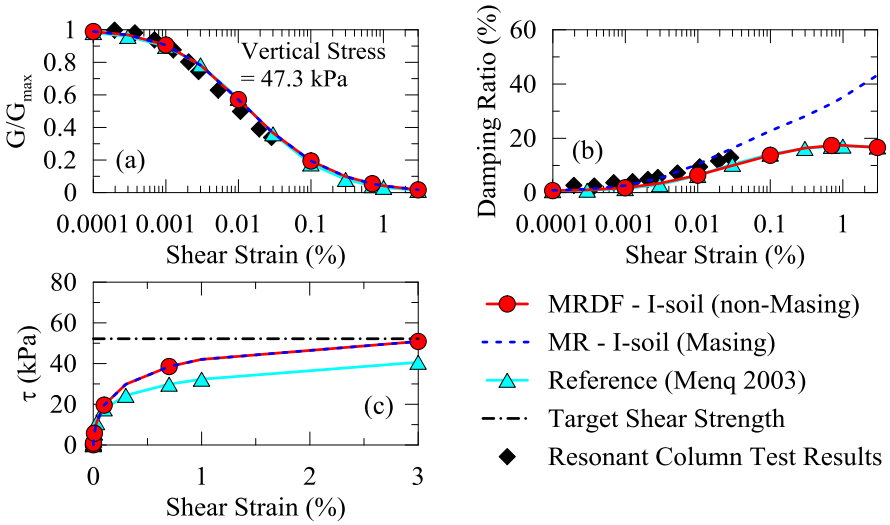

Figure 4: Dynamic curves for I-soil, from resonant column tests and from Menq (2003): (a) Normalized modulus reduction; (b) Damping; and (c) Backbone curves.

Hubler et al. (2017) investigated monotonic constant volume shear response of three gravel materials and found that phase transformation angle was dependent on the particle angularity. It is reported that the gravel material having friction angle of 42˚ (ultimate state) had a phase transformation angle (φ_{pt}) of 32˚, which was used to calculate $\eta_{pt} = \tan(\varphi_{pt})$ for the rockfill material. The average value of $A_0 = 1.0$ was used for the simulations based on the typical values reported by Ghofrani and Arduino (2017) for analogous shear induced volumetric model parameter A_0 used in Dafalias and Manzari (2004). Further study on better characterizing the volumetric response parameters is an ongoing study within the I-soil framework.

Interface between Rockfill and Concrete Face: The connection between the rockfill and the concrete face was modeled based on two different approaches: (1) welded contact which shares the same nodes on the interface and does not allow slippage of concrete face over rockfill, and (2) friction contact which allows the sliding and gapping on the interface, as illustrated in Figure 5. The influence of these interface type on the response of the dam was investigated by comparing the measured response to the computed response. The friction contact obeys the Coulomb friction formulation and the coefficient of friction ($\tan\delta$) was calculated using $tan(\delta) = tan(\frac{2}{3}\varphi')$ (Bowles 1996).

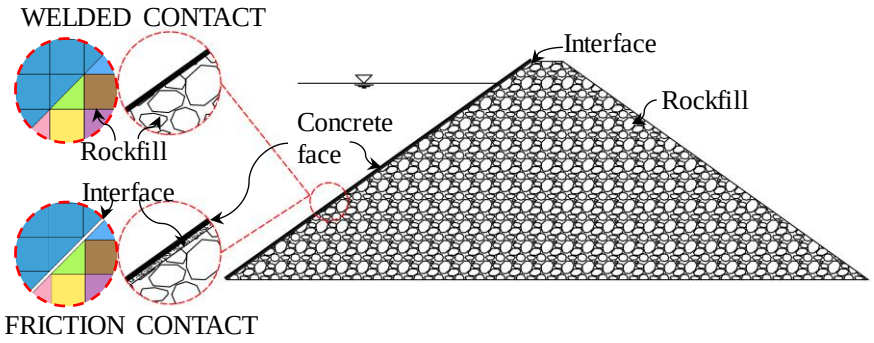

Figure 5: The interface types between the concrete face and the rockfill.

COMPARISON OF MEASURED AND COMPUTED RESULTS

The numerical results, including 5% damped spectral accelerations, bending moment increments and PGA profile, were compared to centrifugal measurements. Figure 6 shows the comparison of computed and measured spectral accelerations (S_a) at locations of A14, A13 and PGA profile for Test 04. The best estimation was obtained when the non-Masing un/reloading and friction contact were utilized. The Masing un/reloading rules significantly underestimated the response spectra, as the magnitude of shaking level increases. This underestimation could be attributed to the overestimation of hysteric damping in the Masing un/reloading rules at large shear strains. The influence of contact type between rockfill and concrete face slab can also be observed in Figure 6. A good agreement between computed and measured spectral accelerations was achieved when friction contact was used. Welded contact caused overestimation at lower periods and underestimation in periods between 0.1 to 0.4 s was observed, particularly at the crest (A14). Computed PGAs were close to measured PGAs until mid-height of the dam, while slight overestimation was seen at the crest. Overall, significant improvement in the response of the model was observed when the non-Masing un/reloading rules and friction contact were utilized in the numerical model.

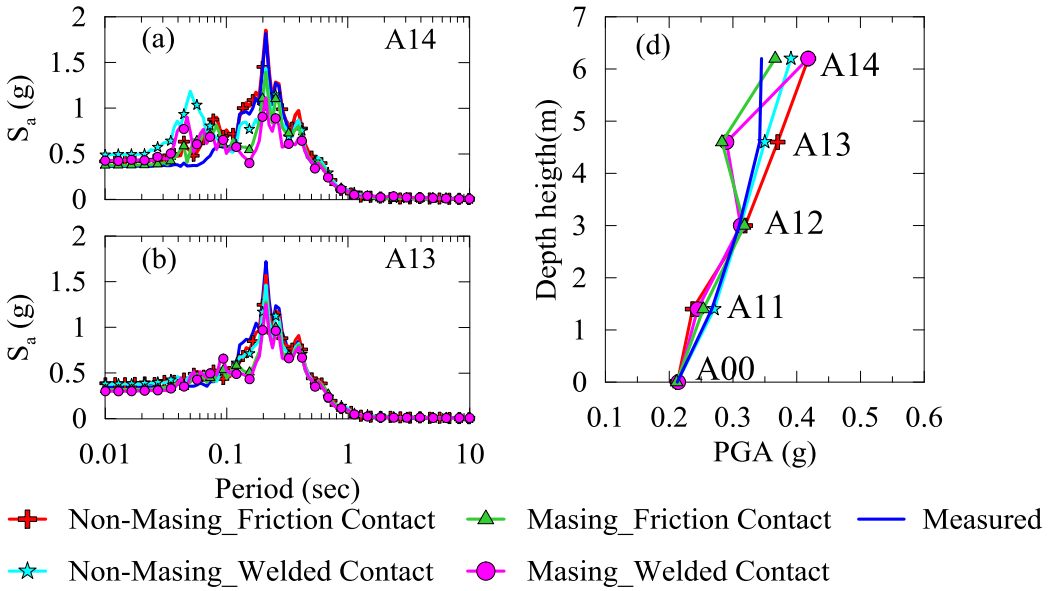

Figure 6: Comparison of recorded and computed spectral accelerations at locations A14 and A13 for Test 04.

The residual spectral accelerations of Test 04 are also calculated to better demonstrate the overall difference between centrifugal measurements and computed estimations that are obtained from non-Masing type un/reloading with frictional interface between rockfill and concrete face case. The residuals spectral accelerations were calculated using $Residual\, S_a = log(S_{a,measured} / S_{a,computed})$. The residual spectral accelerations for the model in which non-Masing type un/reloading rules and friction contact were utilized are presented in Figure 7.

Good estimation of response spectra was achieved in periods between 0.1 to 1 s at almost all the locations. An average residual overestimation of -0,05 (12% overestimation) was observed in periods ranging from 0.01 to 0.03 s in response spectra at all locations except A11 in which an average residual underestimation of 0.04 (9% underestimation) was observed. The average residual overestimation of -0.07 (17% overestimation) was seen in periods between 0.03 to 0.09 s with a maximum difference of -0.26 at location of A32, which means 1.82 times higher than measured S_a (see Figure 7b). In periods between 1 to 10 s, the maximum underestimation of 0.49 and maximum overestimation of -0.67 were observed; however, it can be considered as insignificant because the measured and computed spectral accelerations are small between these periods.

Figure 8 shows the comparison of computed and measured maximum and minimum bending moment increments of the concrete face slab for Test 09. The strain gages provided data were SG1, SG4, SG7, and SG8 (see Figure 1 for the locations). Kim et al. (2011) stated that the bending moments were calculated using $M_p = -(\epsilon_o - \epsilon_i)\frac{(Et^2N^2)}{12(1-\nu^2)}$, where ϵ_o is the strain on the outer face, ϵ_i is the strain on the inner face E is Young's modulus, ν is Poisson's ratio, N is scale factor. The computed bending moment increments for Test 09 showed a very good agreement with centrifugal measurements.

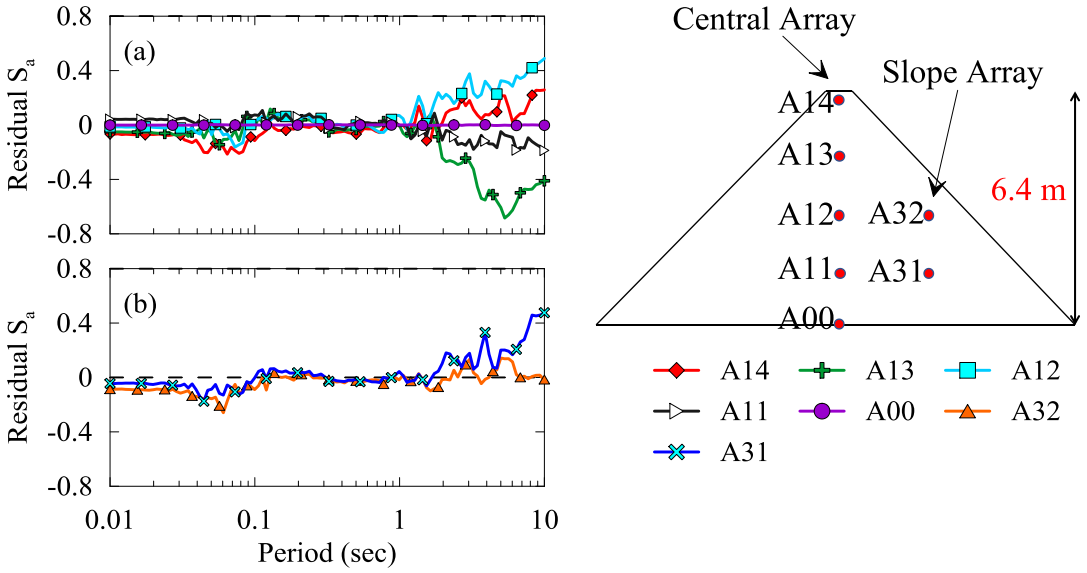

Figure 7: Residual spectral accelerations of Test 04 for the numerical model with non-Masing type hysteretic damping and friction contact: (a) Central array and (b) Slope array.

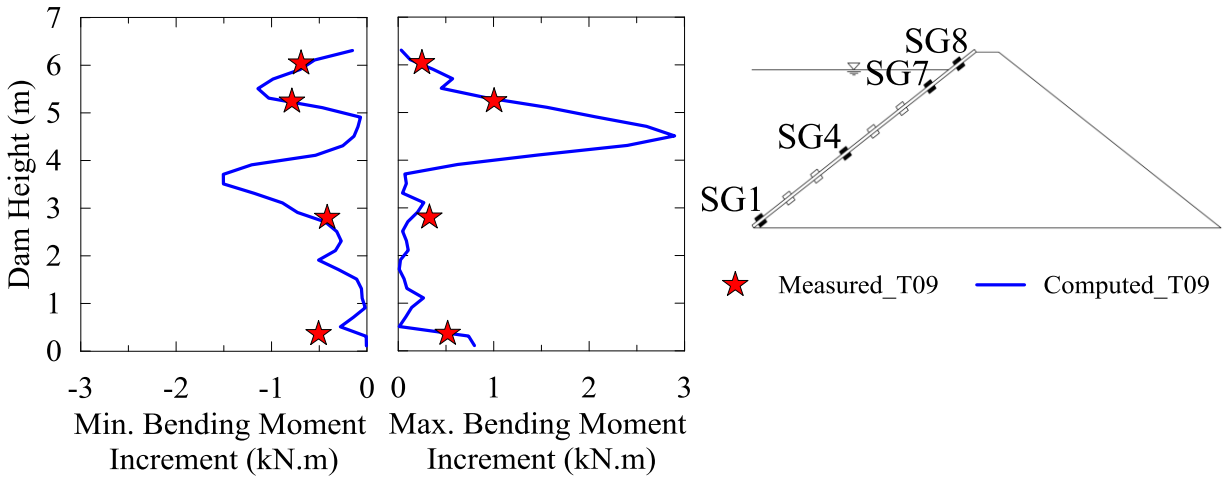

Figure 8: Comparison of computed and measured maximum and minimum bending moment increments on the concrete face slab for the numerical model with non-Masing hysteretic damping formulation and friction contact.

CONCLUSIONS

This study employs a nonlinear dynamic analysis of prototype of a centrifuge model using finite element method and I-soil constitutive model. The dynamic curves of the rockfill material is represented using Menq (2003) correlation. Both Masing and non-Masing type un/reloading rules were utilized and the difference between those rules on the seismic response of a concrete faced rockfill dam were highlighted. The impact of the interface type between the rockfill and the concrete face slab was investigated by employing frictional and welded contact. The computed response of the model was compared to dynamic centrifuge test measurements. The proper representation of the hysteretic damping behavior was found to have significant effects on the seismic response of the dam. The non-Masing type hysteretic damping formulation was

found to result in good agreement with measured spectral accelerations. The Masing type hysteretic damping formulation significantly underestimated the response spectra. It is believed that the overestimation of damping behavior due to Masing rules caused the underestimation of the shear response. The response spectra calculated at the crest was heavily dependent on the connection type between rockfill and the concrete face. The friction contact led to better estimation of spectral accelerations and bending moment increments than welded contact. The computed bending moment increments in the concrete face slab were in good agreement with measured bending moment increments. As a result, the non-Masing un/reloading rules and friction contact resulted in the best estimation of the dam response compared to Masing un/reloading rules and welded contact.

ACKNOWLEDGEMENT

The authors are grateful to Professor Dong-Soo Kim of the Korea Advanced Institute of Science and Technology, Republic of Korea for providing the data recorded during the centrifuge tests. The financial support by the General Directorate of State Hydraulic Works of Turkey for this work is also sincerely appreciated.

REFERENCES

Baltaji, O., Numanoglu, O. A., Veeraraghavan, S., Hashash, Y. M. A., Coleman, J. L., & Bolisetti C. (2017). Non-linear time domain site response and soil structure analysis for nuclear facilities using MOOSE. *Transactions, 24th International Conference on Structural Mechanics in Reactor Technology (SMiRT 24), Busan, South Korea, August 2017*.

Bayraktar, A., & Kartal, M. E. (2010). Linear and nonlinear response of concrete slab on CFR dam during earthquake. *Soil Dynamics and Earthquake Engineering*, *30*(10), 990-1003.

Bowles, J. E. (1996). *Foundation analysis and design*. New York: McGraw-Hill.

Chiang, D. Y., & Beck, J. L. (1994). "A new class of distributed-element models for cyclic plasticity—I. Theory and application." *International journal of solids and structures*, 31(4), 469-484.

Coleman, J., Slaughter, A., Veeraraghavan, S., Bolisetti, C., Numanoglu, O. A., Spears, R., Hoffman, W., & Kurt, E. (2017). *MASTODON Theory Manual* (No. INL/EXT-17-41930). Idaho National Laboratory, Idaho Falls, ID (United States).

Dafalias, Y. F., & Manzari, M. T. (2004). Simple plasticity sand model accounting for fabric change effects. *Journal of Engineering mechanics*, *130*(6), 622-634.

Ghofrani, A., & Arduino, P. (2017). Prediction of LEAP centrifuge test results using a pressure-dependent bounding surface constitutive model. *Soil Dynamics and Earthquake Engineering*, *113*, 758-770.

Groholski, D. R., Hashash, Y. M. A., Kim, B., Musgrove, M., Harmon, J., & Stewart, J. P. (2016). Simplified model for small-strain nonlinearity and strength in 1D seismic site response analysis. *Journal of Geotechnical and Geoenvironmental Engineering*, *142*(9). https://doi.org/10.1061/(ASCE)GT.1943-5606.0001496

Hashash, Y.M.A., Musgrove, M.I., Harmon, J.A., Ilhan, O., Groholski, D.R., Phillips, C.A., and Park, D. (2017) "DEEPSOIL 7.0, User Manual".

Hubler, J. F., Athanasopoulos-Zekkos, A., & Zekkos, D. (2017). Monotonic, Cyclic, and Postcyclic Simple Shear Response of Three Uniform Gravels in Constant Volume Conditions. *Journal of Geotechnical and Geoenvironmental Engineering*, *143*(9), 04017043.

Iwan, W. D. (1967). "On a class of models for the yielding behavior of continuous and

composite systems." *Journal of Applied Mechanics*, 34(3): 612-617.
Jaky, J. (1948). "Pressure in silos." ICSMFE, London 1: 103-107.
Kim, M.-K., Lee, S.-H., Choo, Y. W., & Kim, D.-S. (2011). Seismic behaviors of earth-core and concrete-faced rock-fill dams by dynamic centrifuge tests. *Soil Dynamics and Earthquake Engineering*, *31*(11), 1579–1593. https://doi.org/10.1016/j.soildyn.2011.06.010
LSTC (2009). LS DYNA Keyword User's Manual - Release 971 R4. L. Corporation. Livermore, California.
Marulanda, C., & Marulanda, A. (2015). CFRD: past and present (*). In *25th international congress on large dams*. Stavanger, Norway: International Commission on Large Dams.
Marulanda-Escobar, C., & Marulanda-Posada, A. (2008). Recent experience on design, construction and performance of CFRD dams. In *International Conference on Case Histories in Geotechnical Engineering*. Missouri University of Science and Technology.
Masing G. Eignespannungen und verfestigung beim messing. *In: Second International Congress on Applied Mechanics*, Zurich, Switzerland, 1926, (pp. 332–335).
Menq, F. Y. (2003). *Dynamic Properties of Sandy and Gravelly Soils.* Ph.D, University of Texas at Austin.
Nova, R., & Wood, D. M. (1979). A constitutive model for sand in triaxial compression. *International Journal for Numerical and Analytical Methods in Geomechanics*, *3*(3), 255-278.
Numanoglu, O. A. (2018). Ph.D Thesis in progress. University of Illinois at Urbana Champaign.
Numanoglu, O. A., Hashash, Y. M. A., Cerna-Diaz, A., Olson, S. M., Bhaumik, L., Rutherford, C. J., & Weaver, T. (2017a). Nonlinear 3-D modeling of dense sand and the simulation of a soil-structure system under multi-directional loading. In *Geotechnical Frontiers 2017*. https://doi.org/10.1061/9780784480489.038
Numanoglu, O. A., Musgrove, M., Harmon, J. A., & Hashash, Y. M. A. (2017b). Generalized Non-Masing Hysteresis Model for Cyclic Loading. *Journal of Geotechnical and Geoenvironmental Engineering*, *144*(1), 06017015.
Park, D., Kwak, D. Y., Cho, C. K., & Chun, B. S. (2009). Evaluation of liquefaction potential of port structures with earthquake magnitude adjustment. *Journal of Coastal Research*, 1035-1039.
Phillips, C., & Hashash, Y. M. A. (2009). Damping formulation for nonlinear 1D site response analyses. *Soil Dynamics and Earthquake Engineering*, *29*(7), 1143–1158. https://doi.org/10.1016/j.soildyn.2009.01.004
Richart, F. E., Hall, J. R., & Woods, R. D. (1970). *Vibrations of soils and foundations*. N.J., Prentice-Hall.
Rowe, P. W. (1962). The Stress-Dilatancy Relation for Static Equilibrium of an Assembly of Particles in Contact. Proceedings of the Royal Society of London. Series A, Mathematical and Physical Sciences, (1339), 500.
Seo, M. W., Ha, I. S., Kim, Y. S., & Olson, S. M. (2009). Behavior of concrete-faced rockfill dams during initial impoundment. *Journal of geotechnical and geoenvironmental engineering*, *135*(8), 1070-1081.
Sherard, J. L., & Cooke, J. B. (1987). Concrete-Face rockfill dam: I. Assessment. *Journal of Geotechnical Engineering*, *113*(10), 1096–1112.
Wen, L., Chai, J., Xu, Z., Qin, Y., & Li, Y. (2017). Monitoring and numerical analysis of behavior of Miaojiaba concrete-face rockfill dam built on river gravel foundation in China. *Computers and Geotechnics*, *85*, 230–248. https://doi.org/10.1016/j.compgeo.2016.12.018